

# <sup>3</sup>He-MRI-based measurements of intrapulmonary $p_{O_2}$ and its time course during apnea in healthy volunteers: first results, reproducibility, and technical limitations

Anselm J. Deninger,<sup>1\*</sup> Balthasar Eberle,<sup>2</sup> Michael Ebert,<sup>1</sup> Tino Grossmann,<sup>1</sup> Gorden Hanisch,<sup>3</sup> Werner Heil,<sup>1</sup> Hans-Ulrich Kauczor,<sup>3</sup> Klaus Markstaller,<sup>2,3</sup> Ernst Otten,<sup>1</sup> Wolfgang Schreiber,<sup>3</sup> Reinhard Surkau<sup>1</sup> and Norbert Weiler<sup>2</sup>

<sup>1</sup>Department of Physics, University of Mainz, Staudingerweg 7, D 55099 Mainz, Germany

<sup>2</sup>Department of Anesthesiology, University of Mainz, Langenbeckstr. 1, D 55101 Mainz, Germany

<sup>3</sup>Department of Radiology, University of Mainz, Langenbeckstr. 1, D 55101 Mainz, Germany

Received 11 October 1999; revised 15 December 1999; accepted 22 December 1999

**ABSTRACT:** We applied a recently developed method of following the time course of the intrapulmonary oxygen partial pressure  $p_{O_2}(t)$  during apnea by <sup>3</sup>He MRI to healthy volunteers. Using two imaging series with different interscan times during two breathholds (double acquisition technique), relaxation of <sup>3</sup>He due to paramagnetic oxygen and depolarization by RF pulses were discriminated. In all four subjects, the temporal evolution of  $p_{O_2}$  was found to be linear, and was described by an initial partial pressure  $p_0$  and a decrease rate  $R$ . Also, regional differences of both  $p_0$  and  $R$  were observed. A correlation between  $p_0$  and  $R$  was apparent. Finally, we discuss limitations of the double acquisition approach. Copyright © 2000 John Wiley & Sons, Ltd.

**KEYWORDS:** hyperpolarized gases; magnetic resonance imaging; oxygen partial pressure; lung function; apnea; humans

## INTRODUCTION

In the ventilated airspaces of the lungs, the partial pressure of oxygen is regionally and temporally variable. This results from differences in ventilation-dependent oxygen delivery, and perfusion-dependent oxygen uptake into the blood. Clinicians routinely only measure the resultant  $p_{O_2}$  in mixed expiratory or endexpiratory gas at the mouth, and in arterial and mixed venous blood (for a review see Nunn<sup>1</sup>). From these global measurements, physiological models allow calculation of compartmental  $p_{O_2}$  values in the lungs. However, those values are only model predictions for steady-state conditions, not true  $p_{O_2}$  existing at any point and time in the pulmonary airspace.<sup>2</sup> Up to now,  $p_{O_2}$  within occluded pulmonary segments could only be measured by invasive means.<sup>3</sup> Intrapulmonary  $p_{O_2}$  beyond the level of the bronchi could not be measured at all.

A promising new approach to accessing the alveolar space noninvasively lies in MRI of the lungs with hyperpolarized helium-3. Levels of nuclear polarization which are up to five orders of magnitude higher than thermal (Boltzmann) equilibrium are achieved by optical pumping of <sup>3</sup>He gas. Inhalation of polarized gas allows for MR imaging of upper airways,<sup>4</sup> the tracheobronchial system,<sup>5,6</sup> and alveolar space.<sup>7–9</sup> The diagnostic potential of this method has been demonstrated by various groups.<sup>10–13</sup>

The longitudinal relaxation time  $T_1$  of <sup>3</sup>He in the lung is limited to 10–20 s. The key factor is molecular oxygen, which, via dipolar coupling to the <sup>3</sup>He nuclei, causes rapid depolarization<sup>14</sup> and hence loss of signal. This has been exploited by Eberle *et al.*<sup>15</sup> to compute oxygen concentrations in animal lungs from magnitude <sup>3</sup>He MR images. Values sampled from large alveolar regions correlated well with global endexpiratory measurements from conventional respiratory gas analysis. In a subsequent work, Deninger *et al.*<sup>16</sup> made use of this relaxation effect to determine the local oxygen partial pressure  $p_{O_2}$  in a phantom, a pig and a human volunteer. In order to distinguish more clearly oxygen-induced relaxation from depolarization due to radio frequency (RF) pulses, a double acquisition technique was developed: two series of images are taken under otherwise identical conditions, with only one parameter such as RF voltage or interscan

\*Correspondence to: A. J. Deninger, Institut für Physik, Universität Mainz, D 55099 Mainz, Germany; e-mail: deninger@mail.uni-mainz.de  
Contract/grant sponsor: Deutsche Forschungsgemeinschaft (DFG); contract grant number: TH315/8-1.  
Contract/grant sponsor: Innovationsstiftung des Landes Rheinland-Pfalz.

**Abbreviations used:**  $p_{O_2}$ , partial pressure of oxygen; RF, radio frequency; ROI, region of interest; SNR, signal to noise ratio.

time being varied between series. A simple computation based on MR signal analysis yields the time-dependent p<sub>O2</sub>. In Deninger *et al.*,<sup>16</sup> the temporal evolution of p<sub>O2</sub> during apnea was found to be linear both in an animal and a single human volunteer; hence

$$p_{O_2}(t) = p_0 - Rt \quad (1)$$

holds, where p<sub>0</sub> is the oxygen partial pressure present at the beginning of apnea, and R is the decrease rate. In the animal experiment, a relative accuracy of 3% and 7% was found for p<sub>0</sub> and R, respectively.

In this paper we report on the application of this technique to a sample of four healthy human volunteers, investigating its reproducibility and the limitations of the current double acquisition approach. We confirm the linear approximation of p<sub>O2</sub> given by eq. (1), and show that the initial partial pressure p<sub>0</sub> and the decrease rate R are quantitatively consistent with typical pulmonary function measurements in healthy subjects. We also discuss an apparent correlation between the parameters p<sub>0</sub> and R.

## EXPERIMENTAL

The production of polarized <sup>3</sup>He at the University of Mainz has been reported elsewhere.<sup>17–19</sup> The polarized gas is compressed and stored in uncoated vessels made of special iron-free glass (Schott Glas, Mainz, Germany; volume 360–600 ml, pressure ≈3 bar, initial <sup>3</sup>He polarization ≈40% at flow-rate 8 × 10<sup>18</sup> atoms/s). Transport to the scanner takes place inside a shielded homogenous 0.3 mT guiding field. We use a gas delivery device<sup>15,16</sup> to reproducibly administer a bolus of <sup>3</sup>He into the inspiratory airflow. For all experiments described here, bolus volumes of 180–200 ml were placed at the beginning of a normal inspiratory tidal volume.

### Study subjects

With Ethics Committee approval and informed consent, imaging was performed in four healthy human volunteers (two males of age 24 and 43 years, two females of age 24 and 27 years). They were positioned supine inside the MR scanner, and breathing spontaneously. <sup>3</sup>He was administered via a mouth piece. The intrapulmonary gas volume, in which the volume of <sup>3</sup>He was diluted, was estimated from measurements of the subjects' functional residual capacity and inspired tidal volumes, and ranged between 3 and 4.5 l. During imaging, an inspiratory breathhold (7 and 28–35 s for the first and second imaging series, respectively) was maintained with a nose clamp in place.

### MR imaging protocol

All experiments were carried out on a clinical 1.5 T scanner (Magnetom Vision, Siemens Medical Systems, Erlangen, Germany). A dedicated custom-built coil (Fraunhofer Institut, St. Ingbert, Germany) transmitted and detected MR signals. Imaging was performed by means of a fast low angle shot (FLASH) gradient echo sequence with centric reordering, TR = 11 ms, TE = 4.2 ms, field of view (320 mm)<sup>2</sup>, acquisition matrix 81 × 128, and RF excitation amplitude 5 V (corresponding to flip angles of ~1–2°). In order to suppress influences of gas movement, a single thick slice covering the entire lung (180 mm in coronal orientation) was used.

According to the double acquisition approach described in Deninger *et al.*,<sup>16</sup> two imaging series with different interscan times τ<sub>1</sub>, τ<sub>2</sub> were performed for each subject, with values of τ<sub>1</sub> = 1 s, τ<sub>2</sub> = 4 or 5 s, and a total of eight consecutive scans each.

### Data analysis

Images were analyzed with the program NMRWin (German Cancer Research Center, Heidelberg, Germany). For image analysis, user-defined regions of interest (ROIs) overlying peripheral parts of the lungs were selected to minimize effects of gas movement during apnea from anatomical deadspace (trachea, bronchi) into the ROI, and of gas movement due to cardiogenic mixing. Also, parts of the lungs in which the projection image appears inhomogeneous were avoided (e.g. the basal portions of the lung which contain a projection of the diaphragm).

In these ROIs, mean signal intensities were computed. In order to resolve local variations in p<sub>O2</sub>, which can be assumed to be subtle in healthy individuals, small ROIs of a uniform size of 89 pixel (1.4 cm<sup>2</sup>) were chosen. A noise correction of signal intensities was performed following Gudbjartsson and Patz.<sup>20</sup>

The theory of oxygen determination is described at length in Deninger *et al.*<sup>16</sup> Briefly, the signal intensity A<sub>n</sub> of the n<sup>th</sup> image (n = 1, 2, ..., 7) is normalized to the initial image. Introducing for simplicity a value

$$E_n = \ln\left(\frac{A_n}{A_0}\right) \quad (2)$$

the oxygen partial pressure p<sub>O2</sub>(t'<sub>n</sub>), present at times t'<sub>n</sub> = n(τ<sub>1</sub> + τ<sub>2</sub>) / 2, is computed via

$$p_{O_2}(t'_n) = p_0 - Rt'_n = \xi \frac{E_n(\tau_1) - E_n(\tau_2)}{n(\tau_2 - \tau_1)} \quad (3)$$

Here, ξ denotes the inverse proportionality constant between oxygen partial pressure in bar and <sup>3</sup>He relaxation rate in seconds,<sup>14</sup> i.e. Γ<sub>O2</sub> = p<sub>O2</sub> / ξ. At body temperature, a value of ξ = 2.61 bar × s is to be used.

**Table 1. Subject data**

Study no.	Sex	Age	<sup>3</sup> He bolus/ml		Mean SNR of 1st image	
			Series 1	Series 2	Series 1	Series 2
1	m	24	185	174	38	38
2	m	43	204	199	20	20
3	f	27	199	201	32	29
4	f	24	208	194	17	11

Equation (3) mathematically eliminates flip angle depolarization. The calculation relies upon the assumption of an oxygen partial pressure which decreases in a linear way during short periods of breathholding. The validity of this approximation has been demonstrated in previous experiments.<sup>16</sup> The time course of  $p_{O_2}$  is thus characterized completely, at least early during an apneic period, by an initial partial pressure  $p_0$  and a decrease rate  $R$ . Once these parameters are known, the flip angle  $\alpha$  can be computed by correcting the intensities for oxygen induced relaxation.

Surface relaxation by lung tissue is not considered in this analysis, because a previous investigation<sup>16</sup> has shown this effect to be negligible compared to oxygen induced relaxation and flip angle depolarization.

Error bars were derived according to the empirical law

$$\Delta A \propto \sigma L^{-0.45} \quad (4)$$

described in Deninger *et al.*<sup>16</sup> ( $\sigma$ : noise level of image,  $L$ : ROI size in pixel).

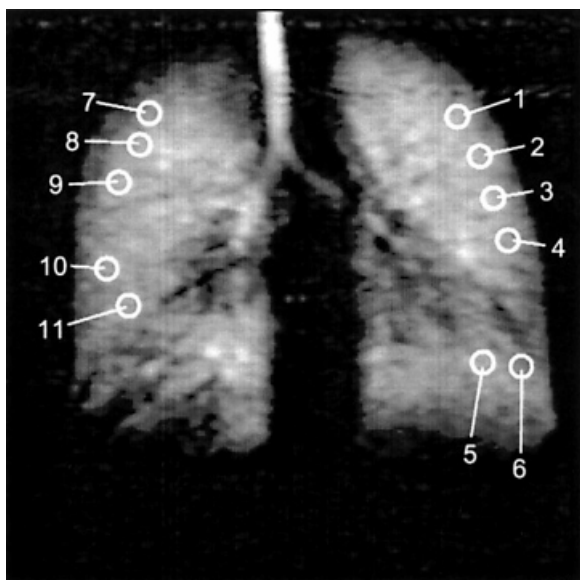


**Figure 1.** Lung image of human volunteer (study 1), and location of analyzed regions of interest (ROIs). In this particular case, the trachea is filled with polarized <sup>3</sup>He (and therefore visible) due to partial expiration prior to breathhold and imaging. Results of intrapulmonary oxygen concentrations in the respective ROIs are listed in Table 2

## RESULTS

In all four subjects, image acquisition was completed successfully and without adverse events. While the volume of the <sup>3</sup>He bolus was reproducible within narrow limits ( $\pm 7 \text{ cm}^3$ , see Table 1), the volume of <sup>3</sup>He distribution in the lung could not be controlled with similar accuracy, because both the lung volume at the start of the test inspiration and the tidal volume varied between acquisitions. Both parameters are difficult to duplicate during spontaneous breathing. Even equal inspiratory volumes can still result in rather different physiological conditions if the residual lung volumes prior to <sup>3</sup>He inhalation vary. Therefore, images of both series were checked for equal appearance of the lungs (i.e. size of lungs, distribution of intensities, position of diaphragm).

According to this criterion, three volunteers were able to breathe reproducibly, whereas in one case (study 4), the lung images of both series were not alike. In the following, results are described separately for each subject.

### Study 1

The lungs of this volunteer were imaged with interscan times of 1 and 5 s, respectively. The average signal to noise ratio (SNR) of a single pixel was 38 for the first images of

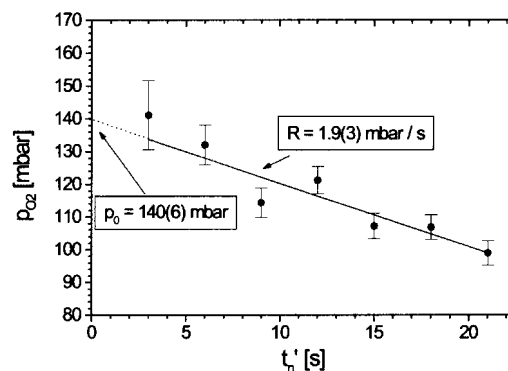


**Figure 2.** Exemplary plot of local intrapulmonary oxygen partial pressure evolution in the lungs of a human volunteer (study 1). The ROI is situated in the cranial left lung (no. 1 in Fig. 1)

**Table 2. Results of study 1**

ROI no.	$p_0$ (mbar)	$R$ (mbar/s)	$\chi^2$ (p.d.f.)	$\alpha$ (degrees)
1	140(06)	1.9(0.3)	1.25	1.8(0.1)
2	141(06)	2.1(0.3)	1.21	1.6(0.1)
3	142(06)	1.6(0.4)	1.60	1.5(0.1)
4	150(07)	1.9(0.4)	1.11	1.2(0.1)
5	156(07)	1.7(0.4)	0.49	1.1(0.2)
6	156(09)	1.8(0.6)	1.47	1.4(0.2)
7	158(08)	2.5(0.5)	1.31	1.6(0.1)
8	153(07)	2.1(0.4)	1.16	1.3(0.1)
9	148(07)	1.3(0.4)	0.58	1.4(0.1)
10	155(09)	1.9(0.6)	0.37	1.1(0.2)
11	178(08)	3.9(0.5)	1.09	0.7(0.3)
Mean (standard deviation)	153(11)	2.3(0.7)		1.3(0.3)

Regional oxygen partial pressure  $p_{O_2}$  in volunteer 1 (male 24 years). The ROIs are depicted in Fig. 1. Listed are values of initial partial pressure  $p_0$ , oxygen decrease rate  $R$ ,  $\chi^2$  p.d.f. of linear fit, and flip angle  $\alpha$  as determined from the  $\tau = 1$  s series. ROI size is 89 pixel (1.4 cm<sup>2</sup>).

either series (see Table 1). Eleven user-defined ROIs were analyzed, the location of which is shown in Fig. 1.

A typical example of a regional oxygen partial pressure evolution is depicted in Fig. 2. Values of  $p_{O_2}$  are plotted as a function of time. The linear decrease is apparent. A similar time course was observed in the other ROIs, albeit with regional differences in both initial pressure  $p_0$  and oxygen decrease rate  $R$ . Results for  $p_0$ ,  $R$ , the  $\chi^2$  of the linear fit per degree of freedom (p.d.f.) and flip angle  $\alpha$  are compiled in Table 2. The mean ( $\pm$ standard deviation) of  $p_0$  is 153(11) mbar. For  $R$ , the respective values are 2.3(0.7) mbar/s.

The data of Table 2 show that high or low values of  $p_0$  are often found with, respectively, high or low values of  $R$ . Indeed, it is interesting to investigate a possible correlation between the two parameters (Fig. 3). Using linear regression analysis, a Pearson's correlation coefficient of  $r = 0.78$  is obtained.

## Study 2

This subject was imaged with interscan times of 1 and 4 s.

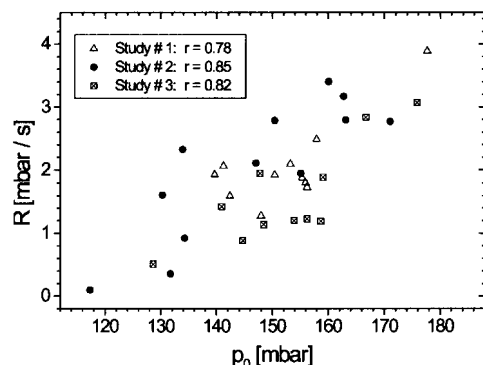


**Figure 3.** Correlation of oxygen decrease rate  $R$  and initial partial pressure  $p_0$  in studies 1–3. Values of Pearson's correlation coefficient are also listed

The initial SNR of both series was 20 (Table 1), which, in this case, was attributed to a lower grade of nuclear polarization of <sup>3</sup>He than in study 1. A total of 12 ROIs were examined. Their distribution is given in Fig. 4, and corresponding results are listed in Table 3. The lower SNR produced larger error bars and, consequently, less accurate fitting results than in study 1. Mean (SD) values of  $p_0$  and  $R$  are 146(17) mbar and 2.0(1.1) mbar/s, respectively. The correlation between these values was even more stringent than in study 1 ( $r = 0.85$ ; see Fig. 3).

## Study 3

This volunteer was examined with interscan times of 1 and 5 s. Mean initial SNR was 32 in the first and 29 in the second series (Table 1). Eleven standard size ROIs were

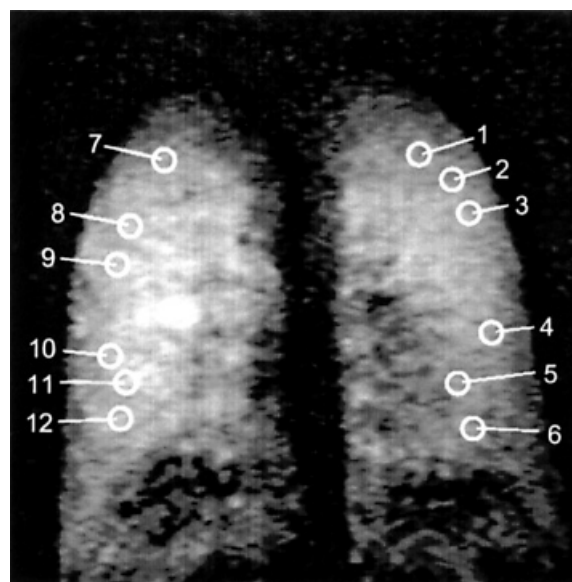


**Figure 4.** Lung image of volunteer 2 and location of ROIs (see Table 3)

**Table 3. Results of study 2**

ROI no.	$p_0$ (mbar)	$R$ (mbar/s)	$\chi^2$ (p.d.f.)	$\alpha$ (degrees)
1	171(18)	2.8(1.4)	0.54	1.7(0.3)
2	163(18)	3.2(1.3)	0.38	1.6(0.2)
3	117(16)	0.1(1.2)	1.14	2.0(0.2)
4	132(17)	0.4(1.4)	0.82	1.6(0.2)
5	150(16)	2.8(1.2)	0.79	1.7(0.2)
6	160(19)	3.4(1.4)	0.50	1.6(0.3)
7	130(16)	1.6(1.2)	1.27	2.0(0.2)
8	134(13)	0.9(1.0)	1.66	1.9(0.2)
9	155(13)	1.9(1.0)	0.92	1.7(0.1)
10	134(13)	2.3(1.0)	0.48	1.9(0.2)
11	163(12)	2.8(0.9)	0.74	1.6(0.2)
12	147(13)	2.1(1.0)	0.25	1.7(0.2)
Mean (standard deviation)	146(17)	2.0(1.1)		1.7(0.2)

Regional oxygen partial pressure  $p_{O_2}$  in volunteer 2 (male 43 years). The ROIs are shown in Fig. 4. ROI size is 89 pixel ( $1.4 \text{ cm}^2$ ).

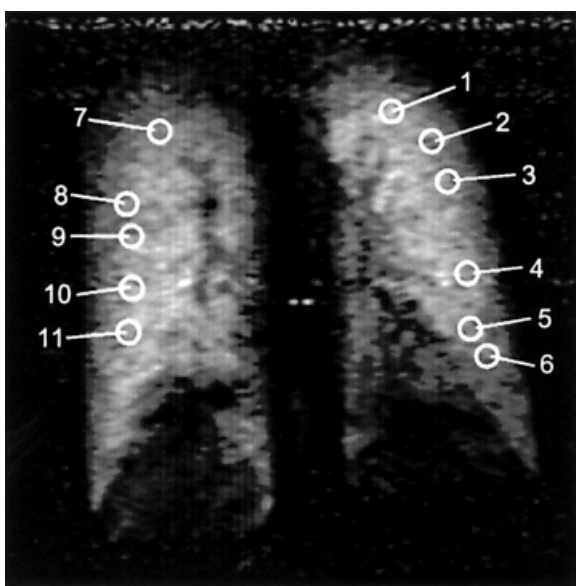


**Figure 5.** Lung image of volunteer 3 and position of ROIs (see Table 4)

analyzed (see Fig. 5 and Table 4). Means (standard deviation) of 153(13) mbar for  $p_0$  and 1.6(0.8) mbar/s for  $R$  were found. The correlation between  $R$  and  $p_0$  is described by a value of  $r = 0.82$  (Fig. 3).

#### Study 4

Two series of images were taken with interscan times of 1 and 5 s. SNR was merely 17 and 11 in the first images of each series. The major flaw of this particular double acquisition series was, however, that the volunteer failed to reproduce her tidal volume with sufficient accuracy to satisfy the requirements of the analysis. Consequently, the lung images and, in particular, the position of the diaphragm in both series, look very different (for demonstration, see Fig. 6). Analysis was therefore restricted to cranial parts of the lungs, which are hardly altered by different levels of inspiration. Within six ROIs (see Table 5), means (standard deviations) of  $p_0$  and  $R$  were 163(20) mbar and 2.3(1.4) mbar/s, respectively, the

**Table 4. Results of study 3**

ROI no.	$p_0$ (mbar)	$R$ (mbar/s)	$\chi^2$ (p.d.f.)	$\alpha$ (degrees)
1	159(10)	1.9(0.6)	0.38	2.2(0.1)
2	159(10)	1.2(0.7)	0.33	1.9(0.1)
3	176(10)	3.1(0.6)	0.92	1.9(0.1)
4	141(09)	1.4(0.6)	1.25	1.9(0.1)
5	156(11)	1.2(0.7)	1.55	2.0(0.1)
6	148(12)	1.1(0.8)	1.77	2.0(0.1)
7	154(10)	1.2(0.6)	0.48	2.1(0.1)
8	129(11)	0.5(0.7)	0.93	2.3(0.1)
9	145(10)	0.9(0.6)	0.94	2.0(0.1)
10	148(09)	1.9(0.6)	1.26	2.0(0.1)
11	167(11)	2.8(0.7)	0.77	1.9(0.1)
Mean (standard deviation)	153(13)	1.6(0.8)		2.0(0.1)

Regional oxygen partial pressure  $p_{O_2}$  in volunteer 3 (female 27 years). Data correspond to ROIs in Fig. 5. ROI size is 89 pixel ( $1.4 \text{ cm}^2$ ).

**Table 5. Results of study 4**

ROI no.	$p_0$ (mbar)	$R$ (mbar/s)	$\chi^2$ (p.d.f.)	$\alpha$ (degrees)
1	177(22)	2.2(1.6)	0.44	1.5(0.3)
2	188(18)	4.2(1.1)	0.32	1.6(0.2)
3	166(19)	3.2(1.3)	0.84	1.6(0.3)
4	137(22)	0.0(1.5)	1.80	1.8(0.3)
5	165(22)	2.4(1.6)	0.84	1.8(0.3)
6	143(21)	1.8(1.3)	1.34	1.8(0.3)
Mean (standard deviation)	163(20)	2.3(1.4)		1.7(0.1)

Regional oxygen partial pressure  $p_{\text{O}_2}$  in volunteer 4 (female 24 years), referring to ROIs in Fig. 6. ROI size is 89 pixel ( $1.4 \text{ cm}^2$ ). Cranial ROIs only were analyzed.

comparatively large uncertainties resulting from the low SNR. Since the amount of inspired room air was not alike, however, intrapulmonary gas composition within both series was different; hence, results are questionable (see Section 4).

## DISCUSSION

This study of healthy human subjects shows that  $^3\text{He}$ -MRI-derived measurements of regional intrapulmonary  $\text{O}_2$  and its time course are well reproducible if certain methodological criteria are fulfilled, such as use of high-grade hyperpolarization, accurate reproduction of  $^3\text{He}$ -inspiration and breathhold, limitation of the analysis to the initial 30–35 s of a breathhold, and therefore a careful choice of interscan times. The oxygen concentration measured at the beginning of a breathhold ( $p_0$ ) is in good agreement with alveolar  $p_{\text{O}_2}$  values determined by the multiple inert gas technique (MIGET): Wagner *et al.*<sup>21</sup> calculated values from 80 to 163 mbar for normal young

subjects breathing room air. One has to take into account, however, that Wagner *et al.* compute steady-state levels of alveolar  $p_{\text{O}_2}$ , whereas the parameter  $p_0$  of our technique reflects an oxygen partial pressure which is present instantaneously after inspiration of fresh air. This explains the somewhat higher  $p_0$  values in our study, the individual mean values of which range from 146 to 163 mbar.

The assumption of a linearly decreasing oxygen concentration during apnea, which is implied in our method of analysis, may require some discussion. Contrary to what would be expected if alveolocapillary  $\text{O}_2$  transfer were a purely physical process, the rate of oxygen transfer is not proportional to the alveolocapillary  $p_{\text{O}_2}$  gradient.<sup>1</sup> The reason is that the chemical association between oxygen and hemoglobin occurs sufficiently slowly to constitute the main limiting factor in the rate of  $\text{O}_2$  transfer from alveolar gas into red blood cells.<sup>22</sup> In other words,  $\text{O}_2$  uptake is *perfusion* limited and not *diffusion* limited. Therefore, after breathing room air, the decrease of  $p_{\text{O}_2}$  in the alveolar space may be approxi-

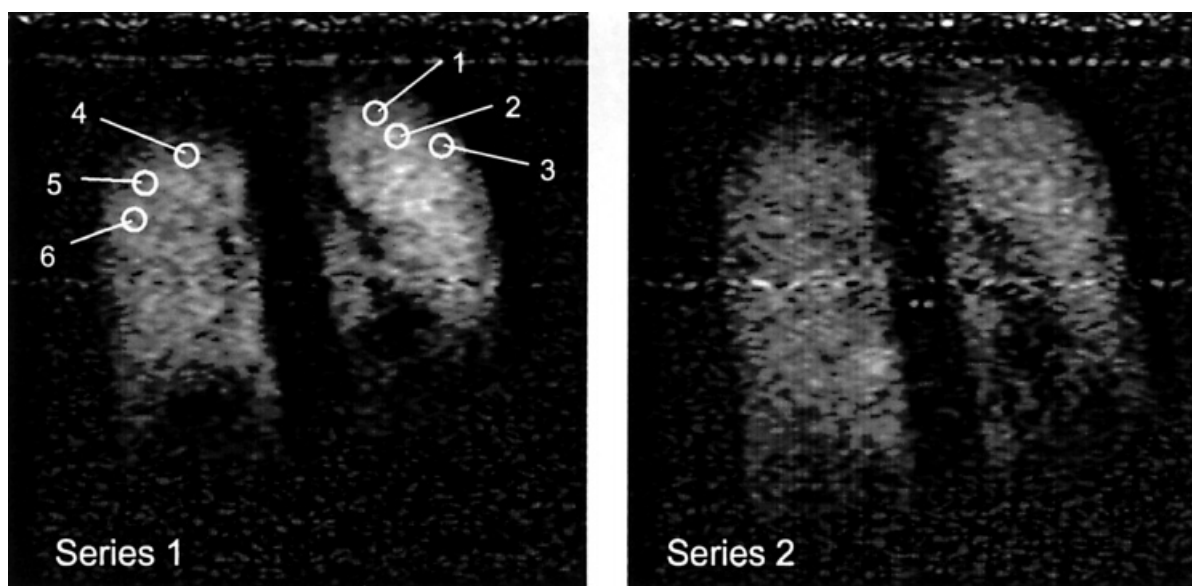


**Figure 6.** Initial images of the two series of the double acquisition experiment in study 4. This volunteer did not reproduce her breath accurately. (Note the different position of the diaphragm in both images.)

mated as linear, at least for the breathhold period until arterial oxygen saturation begins to decrease<sup>23</sup> (beyond 45 s). This condition was readily fulfilled in our healthy subjects during breathholds of less than 35 s duration.

In such a situation, alveolar  $p_{O_2}$  (about 140 mbar during air breathing) approaches the mixed venous  $p_{O_2}$  (normal  $\approx 53$  mbar) within about a minute, if the breathhold is maintained with the upper airways occluded.<sup>1</sup> This global rate of about 87 mbar/min given in the literature is quite close to the regional rates of 1.6–2.3 mbar/s measured in our study, which correspond to 96–138 mbar/min. The residual difference may be explained by a higher than baseline oxygen consumption of our young, alert volunteers. It can thus be surmised that the decrease of the oxygen concentration measured by <sup>3</sup>He-MRI during breathhold in peripheral full-thickness regions of interest predominantly reflects perfusion-driven oxygen uptake into the blood. One additional factor however, particularly in volumes of interest which inadvertently contain significant fractions of dead space, may be the progressive replacement of deadspace gas (higher  $p_{O_2}$ ) by alveolar gas (lower  $p_{O_2}$ ). It is known that during breath holding, alveolar gas may mix with dead space gas as far up as the trachea.<sup>1</sup>

The significant correlation of  $p_0$  with the decrease rate  $R$ , which we observed, may indicate the local matching of ventilation and perfusion. Very effective pulmonary vascular reflexes divert blood flow away (and hence reduce  $R$ ) from poorly ventilated regions with low alveolar  $p_{O_2}$  (and hence, low  $p_0$ ) to well ventilated regions with high alveolar  $p_{O_2}$  (hypoxic pulmonary vasoconstriction, HPV).

However, it cannot be ruled out that the correlation is, at least partly, an artifact of data analysis: A steep or shallow slope of the linear fit (i.e. large or small  $R$ ) may give rise to a large or, respectively, small value of  $p_0$ . Therefore, the application of the fitting routine to noisy data may contribute to the observed correlation. On the other hand, a previous *in vitro* experiment ( $p_{O_2}$  in a silicone bag)<sup>16</sup> correctly yielded high values of  $p_0$  together with zero decrease, i.e. results of  $p_0$  and  $R$  were independent of each other. Future examinations will have to clarify this point.

Flip angles of studies 2–4 are generally consistent, with little variation both within and between subjects. In study 1, however, the mean flip angle is smaller, with a larger variation across the image. Coil loading is known to influence the overall strength of  $B_1$  and thus the mean flip angle, but has negligible effect on the field distribution, so the larger fractional variation remains unexplained.

Experience from this first series of human subjects demonstrates that the double acquisition method is a potentially powerful tool to measure intrapulmonary oxygen partial pressure evolutions, as long as certain limitations are observed. As stressed in Deninger *et al.*<sup>16</sup> one crucial factor is the polarization level of the gas. The

SNR of the last image of the ‘long’ series (i.e. the one with greater interscan time) must be no less than 2–3 to permit evaluation. For typical values of  $p_0$ ,  $R$  and  $\alpha$ , this requires an SNR of about 20 or higher in the first image. If the <sup>3</sup>He polarization is low, this can theoretically still be achieved by increasing the amount of the He bolus, but that will alter the study variable itself ever more, which is respiratory gas composition in the lungs. In this context one should also consider that the uncertainty of any  $p_{O_2}$  data point is directly proportional to the SNR of the corresponding images. These uncertainties, in turn, determine the accuracy of  $p_0$  and  $R$ . Therefore, even higher nuclear polarizations than in the present experiment are desirable if the goal is to clearly resolve very small differences, e.g. cranial–caudal gradients in the distribution of ventilation and perfusion in healthy individuals.

Another important issue for the double acquisition approach is reproducibility of the inspiratory tidal volume. Numerical simulations show that a 20% (40%) variation in this volume (starting from equal lung volumes after expiration, e.g. the free residual capacity) leads to a relative error of 4–7% (8–14%) for  $p_{O_2}$ , depending on the residual lung volume and its oxygen content. There are two interesting aspects to this. First, if the two breaths contain unequal volumes, calculated  $p_{O_2}$  will be closer to the true  $p_{O_2}$  of the series with long intervals, but values will be not quite correct: if the inspired air volume is larger or, respectively, smaller than in the short series, one obtains too high or too low a value. Second, the decrease rate  $R$  should not be affected by the variation in gas composition, as long as oxygen uptake into the blood remains constant. Another more general consequence of pairing non-identical breathholds for  $p_{O_2}$  analysis is different states of lung inflation (see Fig. 6), so that a ROI defined in a first image series may cover a different segment of the lung in the second series.

These systematic effects could be eliminated by performing the entire measurement within one single breathhold. We are currently examining and testing advanced sampling strategies, based on variation of *both* flip angle and interscan time within one imaging series. If proven successful, the single acquisition strategy might be superior, especially for studies of patients with impaired breathing, where reproducibility in two separate series will likely be an even bigger problem.

A further limitation of this oxygen measurement technique is the aforementioned assumption of a linear decrease in oxygen partial pressure. This becomes definitely incorrect if the breathhold is extended long enough for  $p_{O_2}$  to reach equilibrium with the mixed venous  $p_{O_2}$  (about 50–55 mbar), i.e. after about 60 s. The imaging sequence thus has to be completed before this equilibrium ensues, else eqs (1) and (3) become wrong. This has not been observed experimentally, from which we conclude that saturation was not reached in the studies described here.

## CONCLUSION

The study confirmed that <sup>3</sup>He MRI offers the opportunity of a non-invasive assessment of local intrapulmonary oxygen concentrations and their time course during breathhold maneuvers. The method worked reproducibly in this first small series of healthy human volunteers and yielded physiologically plausible results for initial oxygen partial pressures  $p_0$  and decrease rates  $R$ . The observed correlation between  $p_0$  and  $R$  may possibly reflect ventilation-perfusion matching. The current double acquisition approach is limited by the difficulty of reproducing exactly the volume of <sup>3</sup>He distribution within the lungs in both imaging series.

## Acknowledgements

This work was funded by the Deutsche Forschungsgemeinschaft DFG, grant TH315/8-1 and the Innovationsstiftung des Landes Rheinland-Pfalz.

## REFERENCES

- Nunn JF. 1993. *Nunn's Applied Respiratory Physiology*, 4th edn, Butterworth Heinemann, Oxford.
- Riley RL, Lilienthal JL, Proemmel DD and Franke RE. 1946. On the determination of the physiologically effective pressures of oxygen and carbon dioxide in alveolar air. *Am. J. Physiol.* **147**: 191–198.
- Morrell NW, Wignail BK, Biggs T and Seed WA. 1994. Collateral ventilation and gas exchange in emphysema. *Am. J. Crit. Care Med.* **150**: 635–641.
- Bachert P, Schad LR, Bock M, Knopp MV, Ebert M, Großmann T, Heil W, Hofmann D, Surkau R and Otten EW. 1996. Nuclear magnetic resonance imaging of airways in humans with use of hyperpolarized <sup>3</sup>He. *Magn. Res. Med.* **36**: 192–196.
- Chen XJ, Chawla MS, Hedlund LW, Möller HE, MacFall JR and Johnson GA. 1998. MR microscopy of lung airways with hyperpolarized <sup>3</sup>He. *Magn. Res. Med.* **39**: 79–84.
- Viallon M, Cofer GP, Suddarth SA, Möller HE, Chen XJ, Chawla MS, Hedlund LW, Crémillieux Y and Johnson GA. 1999. Functional MR microscopy of the lung using hyperpolarized <sup>3</sup>He. *Magn. Res. Med.* **41**: 787–792.
- Ebert M, Großmann T, Heil W, Otten EW, Surkau R, Leduc M, Bachert P, Knopp MV, Schad LR and Thelen M. 1996. Nuclear magnetic resonance imaging with hyperpolarized <sup>3</sup>He. *Lancet* **347**: 1297–1299.
- MacFall JR, Charles HC, Black RD, Middleton H, Swartz JC, Saam B, Driehuys B, Erickson C, Happer W, Cates GD, Johnson GA and Ravin CE. 1996. Human lung air spaces: potential for MR imaging with hyperpolarized <sup>3</sup>He. *Radiology* **200**: 553–558.
- Darrasse L, Guillot G, Nacher PJ and Tastevin G. 1997. Low-field <sup>3</sup>He nuclear magnetic resonance in human lungs. *C. R. Acad. Sci.* **324**: 691–700.
- Kauczor H-U, Hofmann D, Kreitner K-F, Nilgens H, Surkau R, Heil W, Pottast A, Knopp M, Otten EW and Thelen M. 1996. Normal and abnormal pulmonary ventilation: Visualization at hyperpolarized He-3 MR imaging. *Radiology* **201**: 564–568.
- Kauczor H-U, Ebert M, Kreitner K-F, Nilgens H, Surkau R, Heil W, Hofmann D, Otten EW and Thelen M. 1997. Imaging of the lungs using <sup>3</sup>He MRI: preliminary clinical and experience in 18 patients with and without lung disease. *J. Magn. Res. Imag.* **7**: 538–543.
- De Lange EE, Mugler III JP, Brookeman JR, Knight-Scott J, Truwit JD, Teates CD, Daniel TM, Bogorad PL and Cates GC. 1999. Lung air spaces: MR imaging evaluation with hyperpolarized <sup>3</sup>He gas. *Radiology* **210**: 851–857.
- Saam B, Yablonskiy DA, Gierada DS, Cooper JD, Lefrak SS and Conradi MS. 1999. Measuring diffusivity of <sup>3</sup>He in human lung: preliminary study of patients with emphysema. *Eur. Radiol.* **9**: B22.
- Saam B, Happer W and Middleton H. 1995. Nuclear relaxation of <sup>3</sup>He in the presence of O<sub>2</sub>. *Phys. Rev. A* **52**: 862–865.
- Eberle B, Weiler N, Markstaller K, Kauczor H-U, Deninger A, Ebert M, Grossmann T, Heil W, Lauer LO, Roberts TPL, Schreiber WG, Surkau R, Dick WF, Otten EW and Thelen M. 1999. Analysis of intrapulmonary O<sub>2</sub>-concentrations by magnetic resonance imaging of inhaled hyperpolarized <sup>3</sup>He. *J. Appl. Physiol.* **87**: 2043–2052.
- Deninger AJ, Eberle B, Ebert M, Großmann T, Heil W, Kauczor H-U, Lauer L, Markstaller K, Otten E, Schmiedeskamp J, Schreiber W, Surkau R, Thelen M and Weiler N. 1999. Quantification of regional intrapulmonary oxygen partial pressure evolution during apnea by <sup>3</sup>He MRI. *J. Magn. Res.* **141**: 207–216.
- Eckert G, Heil W, Meyerhoff M, Otten EW, Surkau R, Werner M, Leduc M, Nacher PJ and Scheerer LD. 1992. A dense polarized <sup>3</sup>He target based on compression of optically pumped gas. *Nucl. Instrum. Meth. A* **320**: 53–65.
- Becker J, Heil W, Krug B, Leduc M, Meyerhoff M, Nacher PJ, Otten EW, Prokscha Th, Scheerer LD and Surkau R. 1994. Study of mechanical compression of spin-polarized <sup>3</sup>He gas. *Nucl. Instrum. Meth. A* **346**: 45–51.
- Surkau R, Becker J, Ebert M, Großmann T, Heil W, Hofmann D, Humblot H, Leduc M, Otten EW, Rohe D, Siemensmeyer K, Steiner M, Tasset F and Trautmann N. 1997. Realization of a broad band neutron spin filter with compressed, polarized <sup>3</sup>He gas. *Nucl. Instrum. Meth. A* **384**: 444–450.
- Gudbjartsson H and Patz S. 1995. The Rician distribution of noisy MRI data. *Magn. Res. Med.* **34**: 910–914.
- Wagner PD, Laravuso RB, Uhl RR and West JB. 1974. Continuous distribution of ventilation-perfusion ratios in normal subjects breathing air and O<sub>2</sub>. *J. Clin. Invest.* **54**: 54–68.
- Staub NC, Bishop JM and Forster RE. 1961. Importance of diffusion and chemical blood cells. *J. Appl. Physiol.* **16**: 511.
- Brandt L, Mertzluff F and Dick W. 1989. Verhalten des arteriellen und gemischtvenösen Blutgasstatus in der Initialphase der Intubationsapnoe. *Anaesthesist* **38**: 167–173.